# Correction

**MICROBIOLOGY**

Correction for "The opportunistic marine pathogen *Vibrio parahaemolyticus* becomes virulent by acquiring a plasmid that expresses a deadly toxin," by Chung-Te Lee, I-Tung Chen, Yi-Ting Yang, Tzu-Ping Ko, Yun-Tzu Huang, Jiun-Yan Huang, Ming-Fen Huang, Shin-Jen Lin, Chien-Yu Chen, Shih-Shuen Lin, Donald V. Lightner, Han-Ching Wang, Andrew H.-J. Wang, Hao-Ching Wang, Lien-I Hor, and Chu-Fang Lo, which appeared in issue 34, August 25, 2015, of *Proc Natl Acad Sci USA* (112:10798–10803; first published August 10, 2015; 10.1073/pnas.1503129112).

The authors note that the author name Shih-Shuen Lin should instead appear as Shih-Shun Lin. The corrected author line appears below. The online version has been corrected.

**Chung-Te Lee, I-Tung Chen, Yi-Ting Yang, Tzu-Ping Ko, Yun-Tzu Huang, Jiun-Yan Huang, Ming-Fen Huang, Shin-Jen Lin, Chien-Yu Chen, Shih-Shun Lin, Donald V. Lightner, Han-Ching Wang, Andrew H.-J. Wang, Hao-Ching Wang, Lien-I Hor, and Chu-Fang Lo**

www.pnas.org/cgi/doi/10.1073/pnas.1517100112

# The opportunistic marine pathogen *Vibrio parahaemolyticus* becomes virulent by acquiring a plasmid that expresses a deadly toxin

Chung-Te Lee[a,b,1], I-Tung Chen[a,c,1], Yi-Ting Yang[a,c], Tzu-Ping Ko[d], Yun-Tzu Huang[a], Jiun-Yan Huang[a], Ming-Fen Huang[e], Shin-Jen Lin[a], Chien-Yu Chen[f,g], Shih-Shun Lin[h], Donald V. Lightner[i], Han-Ching Wang[j], Andrew H.-J. Wang[d], Hao-Ching Wang[e,2], Lien-I Hor[b,2], and Chu-Fang Lo[a,c,k,2]

[a]Institute of Bioinformatics and Biosignal Transduction, College of Bioscience and Biotechnology, National Cheng Kung University, Tainan 701, Taiwan; [b]Department of Microbiology and Immunology, College of Medicine, National Cheng Kung University, Tainan 701, Taiwan; [c]Department of Life Science, National Taiwan University, Taipei 104, Taiwan; [d]Institute of Biological Chemistry, Academia Sinica, Taipei 115, Taiwan; [e]Graduate Institute of Translational Medicine, College of Medical Science and Technology, Taipei Medical University, Taipei 110, Taiwan; [f]Genome and Systems Biology Degree Program, National Taiwan University and Academia Sinica, Taipei 115, Taiwan; [g]Department of Bio-Industrial Mechatronics Engineering, National Taiwan University, Taipei 104, Taiwan; [h]Institute of Biotechnology, National Taiwan University, Taipei 104, Taiwan; [i]Aquaculture Pathology Laboratory, School of Animal and Comparative Biomedical Sciences, University of Arizona, Tucson, AZ 85721; [j]Institute of Biotechnology, College of Bioscience and Biotechnology, National Cheng Kung University, Tainan 701, Taiwan; and [k]Center of Bioscience and Biotechnology, National Cheng Kung University, Tainan 701, Taiwan

Edited by John J. Mekalanos, Harvard Medical School, Boston, MA, and approved July 13, 2015 (received for review February 18, 2015)

**Acute hepatopancreatic necrosis disease (AHPND) is a severe, newly emergent penaeid shrimp disease caused by *Vibrio parahaemolyticus* that has already led to tremendous losses in the cultured shrimp industry. Until now, its disease-causing mechanism has remained unclear. Here we show that an AHPND-causing strain of *V. parahaemolyticus* contains a 70-kbp plasmid (pVA1) with a postsegregational killing system, and that the ability to cause disease is abolished by the natural absence or experimental deletion of the plasmid-encoded homologs of the *Photorhabdus* insect-related (Pir) toxins PirA and PirB. We determined the crystal structure of the *V. parahaemolyticus* PirA and PirB (PirA$^{vp}$ and PirB$^{vp}$) proteins and found that the overall structural topology of PirA$^{vp}$/PirB$^{vp}$ is very similar to that of the *Bacillus* Cry insecticidal toxin-like proteins, despite the low sequence identity (<10%). This structural similarity suggests that the putative PirAB$^{vp}$ heterodimer might emulate the functional domains of the Cry protein, and in particular its pore-forming activity. The gene organization of pVA1 further suggested that *pirAB*$^{vp}$ may be lost or acquired by horizontal gene transfer via transposition or homologous recombination.**

shrimp | AHPND | *Vibrio parahaemolyticus* | Pir toxin | virulence plasmid

Since its first outbreak in China in 2009 (1), the newly emergent shrimp disease acute hepatopancreatic necrosis disease (AHPND) (2), originally known as early mortality syndrome, has spread through Southeast Asia to Vietnam, Malaysia, and Thailand to reach as far as Mexico in early 2013 (3, 4). Shrimp production within the AHPND-affected region dropped to ∼60% compared with 2012, and the disease has caused global losses to the shrimp farming industry estimated at more than $1 billion per year (5). In 2013, Tran et al. showed that the causative agent of AHPND was a specific strain of the common Gram-negative halophilic marine bacterium *Vibrio parahaemolyticus* (6). Through some unknown mechanism, this strain had become virulent, and, in infected shrimp, it induced AHPND's characteristic symptoms, i.e., a pale and atrophied hepatopancreas (HP) together with an empty stomach and midgut. Histological examination further showed that AHPND causes sloughing of the HP tubule epithelial cells into the HP tubule lumens (2, 6). Curiously, however, in the initial and acute stage of the disease, although a massive number of bacteria are sometimes found in the stomach chamber in some affected shrimp, there is no significant bacterial colonization of the HP tubule lumen (6). This led Tran et al. to propose that the distinctive pathology of AHPND was caused by a secreted toxin, and this suggestion was supported by the finding that injection of the bacteria-free supernatant of culture broth media into healthy shrimp by reverse gavage can induce the characteristic symptoms of AHPND (6).

Previous studies on AHPND have focused on isolate variations (7), appropriate farming practices (8), or comparisons of draft genome sequences of AHPND-causing strains vs. non-AHPND strains (3, 9–12). In our previous study (9), we used a next-generation sequencing (NGS) platform to sequence and compare three virulent strain and one nonvirulent strain, and found that a large (∼69-kbp) extrachromosomal plasmid was present in all AHPND *V. parahaemolyticus* strains but not in the non-AHPND strains. We also reported that one of the genes (in fact, the operon that comprised ORF50 and ORF51) on this

## Significance

**Since 2009, an emergent shrimp disease, acute hepatopancreatic necrosis disease (AHPND), has been causing global losses to the shrimp farming industry. The causative agent of AHPND is a specific strain of *Vibrio parahaemolyticus*. We present evidence here that the opportunistic *V. parahaemolyticus* becomes highly virulent by acquiring a unique AHPND-associated plasmid. This virulence plasmid, which encodes a binary toxin [*V. parahaemolyticus Photorhabdus* insect-related toxins (PirA$^{vp}$ and PirB$^{vp}$)] that induces cell death, is stably inherited via a postsegregational killing system and disseminated by conjugative transfer. The cytotoxicity of the PirA$^{vp}$/PirB$^{vp}$ system is analogous to the structurally similar insecticidal pore-forming Cry toxin. These findings will significantly increase our understanding of this emerging disease, which is essential for developing anti-AHPND measures.**

Author contributions: C.-T.L., I.-T.C., A.H.-J.W., Hao-Ching Wang, L.-I.H., and C.-F.L. designed research; C.-T.L., I.-T.C., Y.-T.Y., T.-P.K., Y.-T.H., J.-Y.H., M.-F.H., S.-J.L., Han-Ching Wang, and Hao-Ching Wang performed research; C.-T.L., I.-T.C., Y.-T.Y., T.-P.K., Y.-T.H., C.-Y.C., S.-S.L., D.V.L., Hao-Ching Wang, L.-I.H., and C.-F.L. analyzed data; and C.-T.L., I.-T.C., Hao-Ching Wang, L.-I.H., and C.-F.L. wrote the paper.

The authors declare no conflict of interest.

This article is a PNAS Direct Submission.

Freely available online through the PNAS open access option.

Data deposition: The atomic coordinates and structure factors have been deposited in the Protein Data Bank, www.pdb.org [PDB ID codes 3X0T (PirA$^{vp}$) and 3X0U (PirB$^{vp}$)]. The sequence of plasmid pVA1 has been deposited in the GenBank database (accession no. KP324996).

[1]C.-T.L. and I.-T.C. contributed equally to this work.

[2]To whom correspondence may be addressed. Email: gracelow@mail.ncku.edu.tw, h061453@mail.ncku.edu.tw, or wanghc@tmu.edu.tw.

This article contains supporting information online at www.pnas.org/lookup/suppl/doi:10.1073/pnas.1503129112/-/DCSupplemental.

plasmid encoded a homolog of the insecticidal *Photorhabdus* insect-related (Pir) binary toxin PirAB. This homology further suggested that, like PirAB, this plasmidic protein might also exhibit pore-forming activity.

In the present study, the identity of the AHPND virulence factor is determined and confirmed, and the role and importance of the *V. parahaemolyticus* PirAB (PirAB$^{vp}$) toxin in AHPND pathology is demonstrated in its ability to induce AHPND. We propose a structural model of how the PirAB$^{vp}$ complex might act as a pore-forming toxin.

## Results

**Unique Characteristics of AHPND-Causing Strains of *V. parahaemolyticus*.** To identify the critical virulence factors associated with AHPND, we first sequenced the genomes of three AHPND-causing strains (3HP, 5HP, and China) and one non–AHPND-causing strain (S02; Table S1). The contigs were generated from the sequence reads by the de novo genomic assembler Velvet (13), and then Mugsy (14) was used to perform multiple sequence alignments on these closely-related whole genomes to search for AHPND-specific contigs. For this analysis, we also included the complete genome sequence of two other non–AHPND-inducing strains of *V. parahaemolyticus*: human clinical isolate *V. parahaemolyticus* RIMD 2210633 and environmental isolate *V. parahaemolyticus* BB22OP. We retrieved 315 contigs that were found in all three AHPND-causing strains but not in any of the non-AHPND strains. BlastN showed that many of these putative AHPND-specific contigs were homologous to sequences found in plasmids in other *Vibrio* spp. We inferred that these contigs very probably also originated from a plasmid rather than from the *V. parahaemolyticus* chromosomal DNA.

**Analysis of Plasmids Purified from AHPND and Non-AHPND Strains.** To confirm that the unique sequences of the AHPND-causing strains were of plasmidic origin, we purified plasmids from six AHPND and four non-AHPND strains. All the AHPND-causing strains contained from one to five extrachromosomal plasmids (Fig. 1*A*), whereas Southern blot hybridization with a probe (AP2) (9) derived from one of the largest AHPND-specific contigs (12.2 kb) detected a plasmid of ~70 kbp in each of the AHPND-causing strains (Fig. 1*B*). As this strongly suggested that AHPND virulence in *V. parahaemolyticus* is conferred by a common plasmid, we next sequenced the purified plasmids from two strains of AHPND-causing *V. parahaemolyticus* (3HP and M1-1). Our sequencing data revealed that both strains contained a plasmid with a size of ~70 kbp. This APHND-associated plasmid was designated pVA1. Sequence identity of the two pVA1s was 98–99%, and the size also varied slightly.

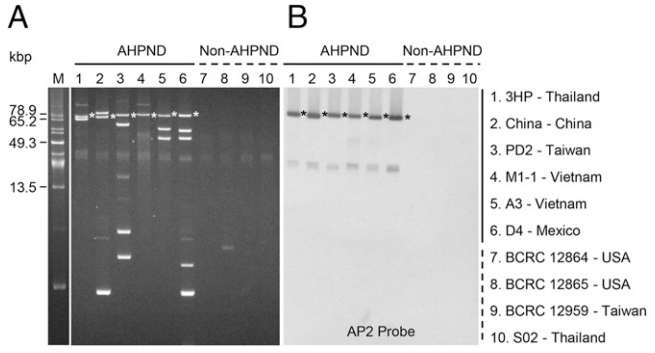


**Fig. 1.** Analysis of plasmids purified from AHPND and non-AHPND strains. (*A*) Uncut plasmids from various AHPND-causing strains (lanes 1–6) and non-AHPND strains (lanes 7–10) after separation in 0.8% agarose gel. The size marker lane (marked "M") shows uncut plasmids from *Pantoea stewartii* SW2 (29). (*B*) Southern blot hybridization signals of the same uncut plasmids after they were transferred to a nylon membrane and probed with alkaline phosphatase-labeled DNA fragments derived from the AP2 amplicon. Asterisks indicate corresponding plasmid bands.

**Sequence Analysis of the APHND-Associated Plasmid pVA1.** Fig. S1*A* shows one of the AHPND-causing strains of *V. parahaemolyticus* (3HP). This strain contains chromosome I (3.3 Mbp), chromosome II (1.9 Mbp), the plasmid pVA1 (70,452 bp), and a 64-kbp non–AHPND-associated plasmid. The pVA1 plasmid was assembled into a single contiguous sequence with a size of 70,452 bp and a G + C content of 45.95%. With the Rapid Annotations using Subsystems Technology online service (15), a total of 59 predicted ORFs were found on the forward strand, whereas 31 predicted ORFs were found on the reverse strand, with sizes ranging from 120 bp to 2,415 bp. The average length of the ORFs was approximately 652 bp, and the gene density was 0.78 per kb (Fig. S1*B*).

The predicted ORFs were annotated by using a protein BLAST (BLASTP) search. Among the 45 putative ORFs with known function (Fig. S1 *B* and *C*, orange), one putative ORF (ORF7) showed homology to the toxin-antitoxin gene *pndA* (16), which is associated with a postsegregational killing (PSK) system. Five putative ORFs resembled transposase (Fig. S1 *B* and *C*, green; ORF15, ORF48, ORF55, ORF57, and ORF68), and three of these (ORF15, ORF48, and ORF55) were identical (ORF48 is in reverse orientation). pVA1 also includes an operon that encodes ORF50 and ORF51, which are homologs (~30% identity) to the pore-forming Pir toxins PirA and PirB (17). We note that, before the emergence of AHPND, this binary insecticidal toxin had not been reported in a marine organism to our knowledge.

**PirAB$^{vp}$ Toxin Leads to Shrimp HP Cell Death and to the Characteristic Sloughing of the Dead Epithelial Cells into the HP Tubules.** Previous reports have shown that, even though AHPND induces massive sloughing of HP cells into HP tubules, there is no sign of any bacteria in the lesions (4, 6, 18). This has led to the suggestion that the observed necrotic effects are caused by some unidentified toxin (6), and we hypothesized that the secreted form of the pVA1-encoded Pir$^{vp}$ toxin was very likely to be responsible.

To test this hypothesis, we first investigated whether AHPND-causing *V. parahaemolyticus* secretes PirA$^{vp}$ and PirB$^{vp}$ into the culture medium. By Western analysis with antibodies against PirA$^{vp}$ and PirB$^{vp}$, we detected secreted PirA$^{vp}$ (12 kDa) and PirB$^{vp}$ (50 kDa) in the AHPND-causing *V. parahaemolyticus* culture medium 1 h after cultivation (Fig. 2*A*).

For the next experiment, we constructed a *pirAB* operon deletion mutant (Fig. 2*B*) of AHPND-causing *V. parahaemolyticus* (Δ*pirAB*$^{vp}$ AHPND-causing *V. parahaemolyticus*) by conjugation of AHPND-causing *V. parahaemolyticus* with *Escherichia coli* S17-1λ*pir* that had been transformed with recombinant pIT009 with the *pirAB*$^{vp}$ operon deletion allele. We also constructed a complementation mutant (Fig. 2*B*) by introducing a recombinant pIT009 with the *pirAB*$^{vp}$ operon into the Δ*pirAB*$^{vp}$ AHPND-causing *V. parahaemolyticus* by conjugation for *in trans* expression of PirAB$^{vp}$ toxin. We confirmed by Western blot analysis that Δ*pirAB*$^{vp}$ AHPND-causing *V. parahaemolyticus* did not produce PirA$^{vp}$ or PirB$^{vp}$ (Fig. 2*C*). The results of challenge tests revealed that the isogenic Δ*pirAB*$^{vp}$ mutant showed a dramatic decrease in virulence and caused no AHPND-like histopathology, whereas both effects were recovered by the complementation mutant that exogenously expressed PirAB$^{vp}$ (Fig. 2 *D* and *E*). These results suggest the PirAB$^{vp}$ toxin plays a critical role in producing the characteristic symptoms of AHPND.

To further explore the toxicity of PirA$^{vp}$, PirB$^{vp}$, and the PirAB$^{vp}$ complex, shrimp were challenged with the recombinant proteins themselves or with two *E. coli* BL21 recombinants that respectively expressed recombinant PirA$^{vp}$ (rPirA$^{vp}$) and rPirB$^{vp}$ (Fig. 2*F*). When reverse gavage was used to directly inject 100 μL

MICROBIOLOGY

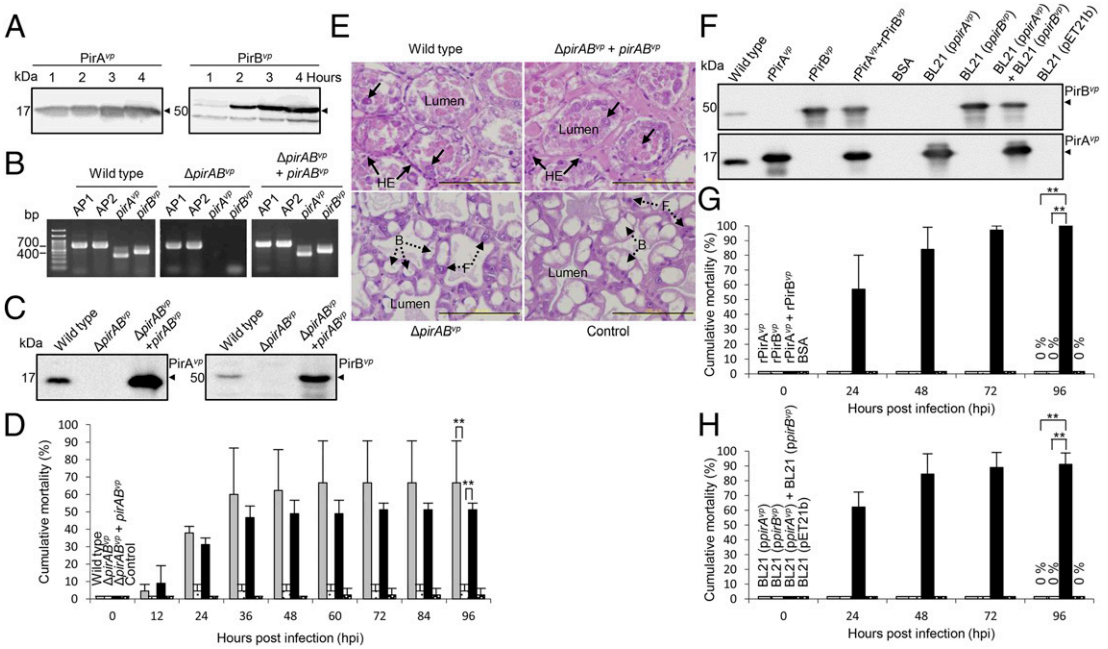


**Fig. 2.** PirAB$^{vp}$ toxin leads to shrimp HP cell death, the characteristic sloughing of the dead epithelial cells into the HP tubules, and mortality within 24 h. (*A*) Western blot analysis with anti-PirA$^{vp}$ and anti-PirB$^{vp}$ antibodies detected PirA$^{vp}$ and PirB$^{vp}$ proteins in the medium of a *V. parahaemolyticus* culture during the log phase of growth (1–4 h). (*B*) PCR confirmation of the AP1, AP2, *pirA*$^{vp}$, and *pirB*$^{vp}$ sequences in the Δ*pirAB*$^{vp}$ and Δ*pirAB*$^{vp}$+*pirAB*$^{vp}$ strains. (*C*) Western blot analysis with anti-PirA$^{vp}$ and anti-PirB$^{vp}$ antibodies shows the presence or absence of PirA$^{vp}$ and PirB$^{vp}$ proteins in the Δ*pirAB*$^{vp}$ and Δ*pirAB*$^{vp}$+*pirAB*$^{vp}$ strains. (*D*) Virulence assay shows cumulative mortalities of shrimp immersed in the WT, Δ*pirAB*$^{vp}$, and the complemented strains. Shrimp immersed in TSB were used as a negative control. Significant differences were determined by unpaired Student *t* test (**$P < 0.005$). (*E*) Sections of the HP from shrimp in the virulence assay were stained with H&E and subjected to histological examination. The typical AHPND signs of sloughed epithelial cells (arrows) and hemocytic encapsulation (HE) were induced by the WT and the complemented strains, whereas shrimp immersed in the Δ*pirAB*$^{vp}$ strain or the TSB control exhibited normal B- and F-cells (broken arrows) without any sloughing of the tubule cells. (Scale bar: 100 μm.) (*F*) To confirm the toxin content used in the per os challenge, Western blot with anti-PirA and anti-PirB probes was used to detect the purified recombinant Pir toxins rPirA$^{vp}$, rPirB$^{vp}$, rPirA$^{vp}$+rPirB$^{vp}$, and the *E. coli* recombinants BL21 (p*pirA*$^{vp}$), BL21 (p*pirB*$^{vp}$), and BL21 (p*pirA*$^{vp}$) + BL21 (p*pirB*$^{vp}$). WT AHPND strain 3HP was used as the positive control, and BSA and the empty vector BL21 (pET21b) were used as the negative controls. (*G* and *H*) Results of per os challenge show cumulative mortalities of shrimp fed with pellets soaked for 10 min in solutions containing (*G*) purified recombinant Pir toxin rPirA$^{vp}$, rPirB$^{vp}$, and rPirA$^{vp}$+rPirB$^{vp}$ and (*H*) the *E. coli* recombinants BL21 (p*pirA*$^{vp}$), BL21 (p*pirB*$^{vp}$), and BL21 (p*pirA*$^{vp}$) + BL21 (p*pirB*$^{vp}$). Shrimp fed with pellets soaked in BSA or in the *E. coli* recombinant with the expression vector only, BL21 (pET21b), was used as the negative controls. Significant differences were determined by unpaired Student *t* test (**$P < 0.005$).

of 2 μM rPirA$^{vp}$, rPirB$^{vp}$, or premixed rPirA$^{vp}$+rPirB$^{vp}$ into shrimp (body weight 1 g), histological examination of HP tissue sections showed that, although rPirA$^{vp}$ caused only minor histological changes, the premixed rPirA$^{vp}$+rPirB$^{vp}$ and the rPirB$^{vp}$ alone induced typical signs of AHPND, including sloughing of the epithelial cells into the HP tubules (Fig. S2*A*). However, when shrimp were challenged by the more natural per os pathway in feeding trials, rPirB$^{vp}$ alone showed no histological effect, whether administered as a protein or via *E. coli* BL21 (Fig. S2 *B* and *C*), whereas mortality was significantly increased only by a mixture of both toxins and by a mixture of both toxin-expressing *E. coli* BL21 recombinants (Fig. 2 *G* and *H*).

**Natural Deletion/Insertion of *pir* Genes.** Further evidence of the importance of the PirAB$^{vp}$ toxin in causing AHPND comes from *V. parahaemolyticus* strain M2-36, which was isolated from a culture pond in Vietnam after an outbreak of AHPND. Although M2-36 gave positive PCR results with primer sets derived from AP1 and AP2 (Fig. S3), it failed to induce AHPND in shrimp that were challenged by immersion (Fig. S4). PCR amplification of a region of the plasmid between AP1 and AP2 produced an amplicon of only ~3,701 bp instead of the expected ~9,116 bp. Southern hybridization confirmed that the amplified region was from an M2-36 plasmid (Fig. S5), and sequencing revealed that the entire *pirAB* operon was missing from this amplicon (Fig. 3). Interestingly, the missing *pirAB* fragment was flanked by two mobile elements: upstream, there was a transposable element protein (transposase) with terminal inverted repeats, whereas the transposase downstream shared 100% sequence identity but was oriented in the opposite direction as the transposase upstream, suggesting that the acquisition of *pirAB*$^{vp}$ by pVA1 or the deletion of *pirAB* from M2-36 might have resulted from a horizontal gene transfer between microorganisms via gene transposition or homologous recombination.

**The pVA1 Plasmid Is the Only Source of the AHPND-Causing Toxin.** To confirm that the pVA1 plasmid was the only source of *pirAB*$^{vp}$, the plasmid needed to be cured, i.e., removed, from the bacterium.

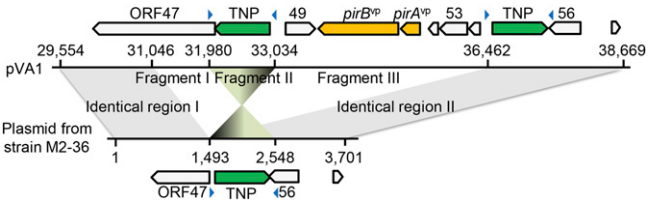


**Fig. 3.** Comparison of pVA1 and the non–AHPND-causing plasmid from strain M2-36 shows the location of the missing DNA fragments. Putative pVA1 ORFs are indicated by the boxes marked with arrows. In the sequence amplified by the AP1-F16/AP2-R1 primer set (Table S2), fragments I and III are absent from the plasmid in the M2-36 strain, whereas fragment II is in reverse orientation. The blue arrowheads represent inverted repeats.

However, in our preliminary trials, we failed to produce any cured clones from more than 20,000 clones that were sensitive to the chloramphenicol acetyltransferase marker. We determined that this was a result of the *pndA* toxin-antitoxin gene, which provides the pVA1 plasmid with a PSK system. When a bacterium contains a PSK$^+$ plasmid, any of the bacterium's progeny that do not inherit this plasmid will die because the stable *pndA* mRNA will be translated to the bactericidal PndA toxin (16). To prevent the PSK effect, *pndA* was therefore deleted by allelic exchange under sucrose stress conditions via conjugation of an AHPND-causing *V. parahaemolyticus* (3HP) with *E. coli* S17-1λ*pir* that had been transformed with the recombinant suicide vector pDS132-Δ*pndA*$^{vp}$. After *pndA* deletion, the pVA1 plasmid was successfully cured from the pVA1 Δ*pndA*$^{vp}$ 3HP mutant by using a high concentration of the plasmid curing agent acridine orange. As shown in Fig. 4*A*, the 64-kb non-AHPND plasmid was still present in the pVA1-cured strain, and the bacterial growth of the cured strain was unaffected after undergoing the curing process (Fig. S6). However, the virulence of the pVA1-cured derivative was greatly impaired (Fig. 4 *B–D*), and histopathological examination of shrimps infected with this pVA1-cured strain showed normal HP tissue morphology (Fig. 4*E*). We also found that reintroduction of the PirAB$^{vp}$ toxin via exogenous expression (by introducing a recombinant pIT009 with *pirAB*$^{vp}$ operon into the pVA1-cured strain) restored virulence and the cytopathic effects (Fig. 4 *B–E*). These data suggested that *pirAB*$^{vp}$, irrespective of other plasmidic factors of pVA1, was sufficient to produce the symptoms associated with AHPND.

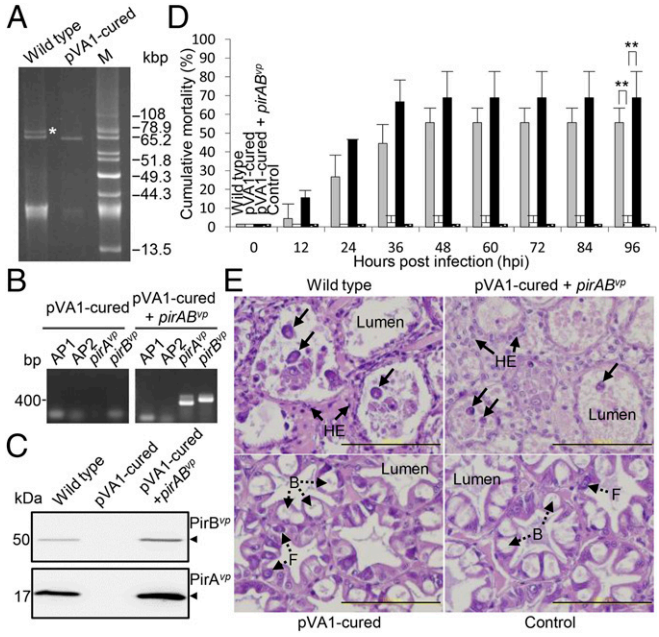


**Fig. 4.** AHPND virulence is abolished in the pVA1-cured derivative and recovered by *in trans* expression of PirAB$^{vp}$. (*A*) Uncut plasmid profiles of the 3HP AHPND WT strain and its pVA1-cured derivative. Plasmid DNAs extracted from the respective strains were separated in a 0.8% agarose gel. The band corresponding to the plasmid pVA1 is indicated by an asterisk. M, uncut plasmids from *P. stewartii* SW2 as size markers. (*B*) PCR confirmation of the AP1, AP2, *pirA*$^{vp}$, and *pirB*$^{vp}$ sequences in the pVA1-cured and pVA1-cured+*pirAB*$^{vp}$ strains. (*C*) Western blot analysis with anti-PirA$^{vp}$ and anti-PirB$^{vp}$ antibodies to show the presence or absence of PirA$^{vp}$ and PirB$^{vp}$ proteins in the pVA1-cured and pVA1-cured+*pirAB*$^{vp}$ strains. (*D*) Virulence assay shows cumulative mortalities for shrimp immersed in the WT, pVA1-cured, and pVA1-cured+*pirAB*$^{vp}$ strains. Shrimp immersed in tryptic soy broth (TSB) were used as a negative control. Significant differences compared with the negative control were determined by unpaired Student *t* test (**$P < 0.005$). (*E*) Sections of the HP from shrimp in the virulence assay were stained with H&E and subjected to histological examination. The typical AHPND signs of sloughed epithelial cells (arrows) and hemocytic encapsulation (HE) of the hepatopancreatic tubules were observed in the shrimp immersed in the WT and pVA1-cured+*pirAB*$^{vp}$ strains, whereas normal B- and F-cells without any sloughing of the tubule cells (broken arrows) were seen in the shrimp immersed in the pVA1-cured strain and TSB control. (Scale bar: 100 μm.)

**The Combined Structural Topology of PirA$^{vp}$/PirB$^{vp}$ Resembles That of the Cry Insecticidal Toxins Even Though the Shared Sequence Identity Is Low.** For the original *Photorhabdus* PirAB insecticidal toxin to be effective, both components needed to be coexpressed (17), which suggested that the two proteins might form a binary complex. We found that PirA$^{vp}$ and PirB$^{vp}$ interacted to form a complex in vitro (Fig. 5*A*), and this PirA$^{vp}$/PirB$^{vp}$ complex was detected in the supernatant of a bacterial culture in midlog phase (Fig. 5*B*). In the same supernatant, we also observed a strong signal for PirB$^{vp}$ but not PirA$^{vp}$.

As the crystal structures of the components of the *Photorhabdus* binary PirAB insecticidal toxin are unknown and because, in any case, there is genetic distance between the *pirAB* coding region of the *V. parahaemolyticus* strains vs. *Photorhabdus* and the other *pirAB*-harboring bacterial species (Fig. S7), we crystallized PirA$^{vp}$ and PirB$^{vp}$ and used X-ray crystallography to determine their respective structures (Fig. S8 and Table S3). The overall structural topology of PirA$^{vp}$/PirB$^{vp}$ is very similar to that of the *Bacillus* Cry insecticidal toxin-like proteins, even though their shared sequence identity is less than 10% (Fig. 5*C*). This similarity suggested how the putative PirAB$^{vp}$ heterodimer might emulate the functional domains of the Cry protein (Fig. 5*D*), with the N terminal of PirB$^{vp}$ corresponding to Cry domain I (pore-forming activity), the C-terminal corresponding to Cry domain II (receptor binding), and PirA$^{vp}$ corresponding to Cry domain III, which is thought to be related to receptor recognition and membrane insertion (19–21). If this predicted functionality is correct, PirAB$^{vp}$ might induce cell death by forming ionic pores in the cell membrane by using a Cry insecticidal toxin-like mechanism.

## Discussion

We have shown here that the characteristic symptoms of AHPND are caused by the binary insecticidal toxin homologs PirA$^{vp}$ and PirB$^{vp}$, and that these two proteins are encoded by the pVA1 plasmid. This plasmid was found in all six of the AHPND-causing strains isolated from diseased shrimp in several Asian countries and Mexico (Fig. 1). Although virulence plasmids have been reported in several *Vibrio* spp. that are pathogenic for aquatic animals (22–24), plasmid prevalence in *V. parahaemolyticus* is usually less than 25%, and plasmid size typically ranges from 2.4 kb to 23.0 kb (25), which is much smaller than pVA1 and the other non-AHPND plasmids that were found in the AHPND-causing strains. Another interesting difference is that, unlike other fish-pathogenic *Vibrio* species, in which the plasmids contribute to virulence via a plasmid-encoded iron acquisition system (22) or confer resistance against the serum killing effect to overcome host defenses (23), the virulence plasmids of *V. parahaemolyticus* produce toxins that immediately destroy the host cells. We also note that the insecticidal Pir toxins/homologs currently described from bacterial species such as *Photorhabdus* and *Xenorhabdus* have all been found in the bacterial chromosomes (FM162591.1, FN667742.1, and FO704550.1), whereas PirAB$^{vp}$ is the only toxin to be encoded by a plasmid.

It was reported previously that both PirA and PirB needed to be present to induce mortality in insect larvae (17), and now that this binary insecticidal toxin homolog has been found in a marine organism, it likewise seems that both PirA$^{vp}$ and PirB$^{vp}$ are necessary to produce the characteristic symptoms of AHPND (Fig. 2 *G* and *H* and Fig. S2 *B* and *C*).We note, however, that, when challenged by reverse gavage, the PirB$^{vp}$ toxin alone was

MICROBIOLOGY

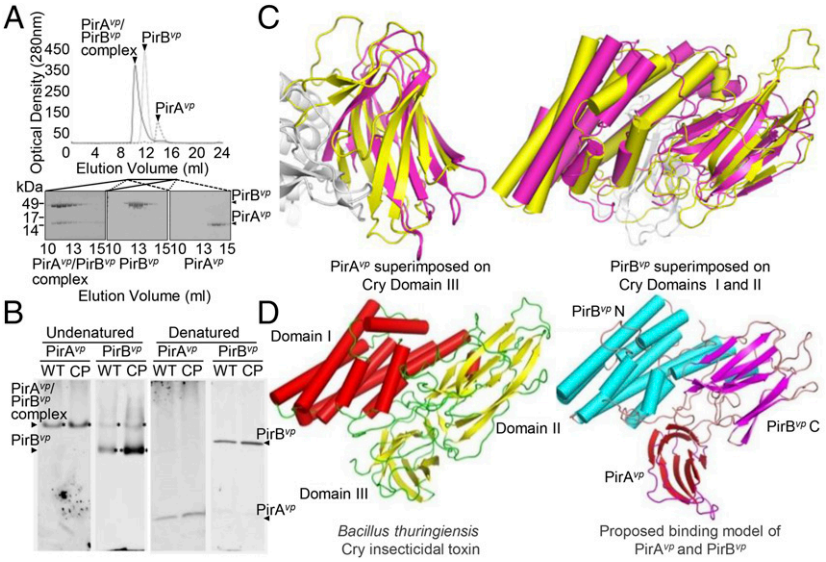


**Fig. 5.** Formation of the PirAB$^{vp}$ complex in vitro and in vivo, and a proposed binding model that suggests a functional similarity between PirAB$^{vp}$ and the Cry proteins. (*A*) When purified PirA$^{vp}$, PirB$^{vp}$, and a PirA$^{vp}$/PirB$^{vp}$ mixture were analyzed separately by using a Superose 16 gel filtration column (GE Healthcare), we found that, for the PirA$^{vp}$/PirB$^{vp}$ mixture, both proteins were eluted faster than the individual proteins on their own. This suggests that PirA$^{vp}$ and PirB$^{vp}$ have formed a complex. (*B*) In the supernatant from a midlog-phase culture of the WT and the pVA1-cured+*pirAB*$^{vp}$ (CP) strains, PirB$^{vp}$ was found in a complex with PirA$^{vp}$ and as a monomer, whereas PirA$^{vp}$ was only detected in the complex. Immunoblotting was performed with anti-PirA$^{vp}$ or anti-PirB$^{vp}$ antibody under undenatured, native PAGE conditions (*Left*). The denatured SDS/PAGE (β-mercaptoethanol; *Right*) confirmed that PirA$^{vp}$ and PirB$^{vp}$ were present in the culture medium. (*C*) Structural comparison of PirA$^{vp}$ and PirB$^{vp}$ with Cry. (*Left*) PirA$^{vp}$ (magenta) is superimposed on domain III of Cry (yellow). (*Right*) PirB$^{vp}$ (magenta) is compared with domains I and II of Cry. PirA$^{vp}$ has an rmsd of 3.2 Å for 88 matched Cα atoms in CRY domain III, and PirB$^{vp}$ superimposes with Cry domain I and II with an rmsd of 2.8 Å for 320 matched Cα atoms. (PDB ID codes: PirA$^{vp}$, 3X0T; PirB$^{vp}$, 3X0U). (*D*) A putative model of the PirAB$^{vp}$ heterodimer was constructed by superimposing PirA$^{vp}$ on domain III of Cry and PirB$^{vp}$ on domains I and II. (*Left*) Cry toxin shown for comparison (PDB ID codes for Cry, 1CIY and ref. 30).

able to induce AHPND-like histological signs (Fig. S2*A*). Reverse gavage is a challenge method commonly used in shrimp to analyze toxicity because, even though it is stressful to the animal, the amount of injected toxin can be quantified, and the mortalities associated with each dosage can be precisely compared. In the present case, in which our per os feeding protocol also ensured that the experimental animals were challenged with comparable dosages, the reason for the observed discrepancy in the toxicity of PirB$^{vp}$ is not clear, but it is presumably related to the different physiological conditions, especially the different enzymes, that would be encountered on the two respective challenge pathways. Meanwhile, as ingestion of AHPND-causing *V. parahaemolyticus* is probably the natural route of infection, it seems likely that the results of the oral feeding challenge are more reliable and more closely represent reality compared with the reverse gavage results, and we therefore tentatively conclude that PirA$^{vp}$ and PirB$^{vp}$ are both required to induce AHPND.

Our results show that the pVA1 plasmid contains a cluster of conjugative transfer genes and two plasmid mobilization genes (Fig. S1 *B* and *C*), which suggests that pVA1 may be a self-transmissible plasmid. When combined with the *pndA* PSK system, this ensures that the plasmid is inherited during bacterial replication, and, in this way, the pVA1 plasmid is passed on to subsequent generations of AHPND-causing *V. parahaemolyticus*. Indeed, as noted earlier (*Results*), we could not obtain any plasmid-cured derivative until the *pndA* gene was deleted. (This result also confirmed that the *pndA* in pVA1 was functional.) Taken together, these two features, i.e., the *pndA* PSK system and the conjugative transfer gene cluster, suggest that the AHPND virulence plasmid might be disseminated via conjugation and then become permanently inheritable in the recipient. The high homology (99~100% identity) of the nucleotide sequences between pVA1 (KP324996) and two corresponding plasmids from the AHPND strains M1-1 and A/3, pVAM1-1 and pVPA3-1 (NC_025152), respectively, further supports the notion that these plasmids—and by extension, all the APHND-causing plasmids—might have originated from the same ancestor.

As for the bacterium itself, Kongrueng et al. found that several AHPND *V. parahaemolyticus* strains isolated from southern Thailand were serologically similar, had closely related pulsed field gel electrophoresis DNA profiles, and possessed the same repertoire of virulence factors (26). This led them to postulate that all these strains might have originated from a single clone. However, it is hard to generalize from this evidence alone because, although all of these strains were isolated from different locations, these locations were all in a single geographic area and lacked geographic diversity. Other reports that have focused on characterizing different AHPND-causing strains have also isolated samples from farms within a single locality (7, 18). To properly address this question, a phylogenetic analysis of various AHPND strains with a wide geographic diversity will be necessary. Until then, it remains unclear whether the different AHPND strains arose from the acquisition of pVA1 by a single *V. parahaemolyticus* ancestor (monophyletic origin) or by several different *V. parahaemolyticus* ancestors (polyphyletic origin).

We postulate that the cytotoxicity of PirA$^{vp}$ and PirB$^{vp}$ can be explained by their crystal structures. Structural alignment shows that PirA$^{vp}$ corresponds to domain III of the *Bacillus thuringiensis* Cry toxin and PirB$^{vp}$ corresponds to domains I and II (Fig. 5*D*). Functionally, Cry toxin induces cell death by undergoing a series of processes that include receptor binding, oligomerization, and pore forming (19, 20). In the case of *B. thuringiensis* Cry1A toxin, domain III first interacts with the GalNAc sugar on the aminopeptidase N (APN) receptor and facilitates further binding of domain II to another region of the same receptor (19–21). This binding promotes localization and concentration of the activated toxins. The APN-bound Cry toxin subsequently binds to another receptor, cadherin, which facilitates the proteolytic cleavage of

its domain Iα1 helix. This cleavage induces the formation of Cry oligomer, which has pore-forming activity (19–21). Interestingly, when Cry toxin binds only to cadherin, it triggers an alternative signal transduction pathway. By activating protein G and adenylyl cyclase, cellular cAMP concentration is increased and protein kinase A is activated. This will destabilize the cytoskeleton and ion channels on the membrane, and induce cell death (27, 28). As the structural similarities suggest that the $PirA^{vp}/PirB^{vp}$ system uses a similar strategy to kill cells, the first step to explore this possibility will be to identify cell receptors that might interact with the $PirA^{vp}/PirB^{vp}$ heterodimer. Given that $PirAB^{vp}$ toxin induces cell death in the HP but not in the stomach, it seems very likely that these putative $PirAB^{vp}$ receptors will be found exclusively in the HP and any other $PirAB^{vp}$ toxin-sensitive organs.

## Materials and Methods

The detailed protocols for NGS, multiple sequence alignment, plasmid isolation, Southern blotting, construction of mutants and complemented strains, plasmid-cured derivative isolation, immersion challenge test, histopathology examination, reverse gavage injection, per os challenge, purification of recombinant Pir protein, gel filtration, protein crystallization, native PAGE analysis, and Western blotting as well as the information of bacterial strains and primers used, are provided in *SI Materials and Methods*.

**ACKNOWLEDGMENTS.** The four *V. parahaemolyticus* strains, 3HP, 5HP, China, and S02 were provided by Dr. Timothy W. Flegel, Dr. Kallaya Sritunyalucksana, and Dr. Siripong Thitamadee. We thank the staff of beamlines BL13B1 and 13C1 at the Radiation Research Center in Hsinchu, Taiwan, for their help in X-ray crystal data collection and Paul Barlow for his helpful criticism of the manuscript. This work was financially supported by the Ministry of Education, Taiwan, Republic of China, under National Cheng Kung University Aim for the Top University Project Promoting Academic Excellence and Developing World Class Research Grant D103-38A01; National Science Council (MSC) of Taiwan Grants NSC 103-2321-B-006-014 and NSC 103-2622-B-006-008; Ministry of Science and Technology (MOST) Grants MOST 103-2313-006-005-MY2, MOST 103-2622-B-006-012-CC1, and MOST 103-2633-B-006-004; Council of Agriculture, Executive Yuan Grants G103-B032 and G103-b329; and the Chen Jie Chen Scholarship Foundation.

1. NACA-FAO (2011) *Quarterly Aquatic Animal Disease Report (Asia and Pacific Region), 2011/2, April-June 2011* (NACA, Bangkok).
2. Lightner DV, Redman RM, Pantoja CR, Noble BL, Tran L (2012) Early mortality syndrome affects shrimp in Asia. *Global Aquaculture Advocate* 15:40.
3. Gomez-Gil B, Soto-Rodríguez S, Lozano R, Betancourt-Lozano M (2014) Draft genome sequence of *Vibrio parahaemolyticus* Strain M0605, which causes severe mortalities of shrimps in Mexico. *Genome Announc* 2(2):e00055-14.
4. Nunan L, Lightner D, Pantoja C, Gomez-Jimenez S (2014) Detection of acute hepatopancreatic necrosis disease (AHPND) in Mexico. *Dis Aquat Organ* 111(1):81–86.
5. FAO Fisheries and Aquaculture (2013) *Report of the FAO/MARD Technical Workshop on Early Mortality Syndrome (EMS) or Acute Hepatopancreatic Necrosis Syndrome (AHPNS) of Cultured Shrimp (under TCP/VIE/3304).* rep. no. 1053, Hanoi, Viet Nam, 25–27 June 2013. Available at www.fao.org/docrep/018/i3422e/i3422e.pdf. Accessed July 28, 2015.
6. Tran L, et al. (2013) Determination of the infectious nature of the agent of acute hepatopancreatic necrosis syndrome affecting penaeid shrimp. *Dis Aquat Organ* 105(1):45–55.
7. Joshi J, et al. (2014) Variation in *Vibrio parahaemolyticus* isolates from a single Thai shrimp farm experiencing an outbreak of acute hepatopancreatic necrosis disease (AHPND). *Aquaculture* 428–429:297–302.
8. De Schryver P, Defoirdt T, Sorgeloos P (2014) Early mortality syndrome outbreaks: A microbial management issue in shrimp farming? *PLoS Pathog* 10(4):e1003919.
9. Yang YT, et al. (2014) Draft genome sequences of four strains of *Vibrio parahaemolyticus*, three of which cause early mortality syndrome/acute hepatopancreatic necrosis disease in shrimp in China and Thailand. *Genome Announc* 2(5):e00816-14.
10. Kondo H, et al. (2014) Draft genome sequences of six strains of *Vibrio parahaemolyticus* isolated from early mortality syndrome/acute hepatopancreatic necrosis disease shrimp in Thailand. *Genome Announc* 2(2):e00221–e14.
11. Gomez-Jimenez S, et al. (2014) High-quality draft genomes of two *Vibrio parahaemolyticus* strains aid in understanding acute hepatopancreatic necrosis disease of cultured shrimps in Mexico. *Genome Announc* 2(4):e00800–e00814.
12. Han JE, Tang KFJ, Tran LH, Lightner DV (2015) *Photorhabdus* insect-related (Pir) toxin-like genes in a plasmid of *Vibrio parahaemolyticus*, the causative agent of acute hepatopancreatic necrosis disease (AHPND) of shrimp. *Dis Aquat Organ* 113(1):33–40.
13. Zerbino DR, Birney E (2008) Velvet: Algorithms for de novo short read assembly using de Bruijn graphs. *Genome Res* 18(5):821–829.
14. Angiuoli SV, Salzberg SL (2011) Mugsy: Fast multiple alignment of closely related whole genomes. *Bioinformatics* 27(3):334–342.
15. Aziz RK, et al. (2008) The RAST Server: Rapid Annotations using Subsystems Technology. *BMC Genomics* 9:75.
16. Nielsen AK, Thorsted P, Thisted T, Wagner EGH, Gerdes K (1991) The rifampicin-inducible genes srnB from F and pnd from R483 are regulated by antisense RNAs and mediate plasmid maintenance by killing of plasmid-free segregants. *Mol Microbiol* 5(8):1961–1973.
17. Waterfield N, Kamita SG, Hammock BD, ffrench-Constant R (2005) The *Photorhabdus* Pir toxins are similar to a developmentally regulated insect protein but show no juvenile hormone esterase activity. *FEMS Microbiol Lett* 245(1):47–52.
18. Soto-Rodriguez SA, Gomez-Gil B, Lozano-Olvera R, Betancourt-Lozano M, Morales-Covarrubias MS (2015) Field and experimental evidence of Vibrio parahaemolyticus as the causative agent of acute hepatopancreatic necrosis disease of cultured shrimp (Litopenaeus vannamei) in Northwestern Mexico. *Appl Environ Microbiol* 81(5):1689–1699.
19. Soberón M, et al. (2010) Pore formation by Cry toxins. *Adv Exp Med Biol* 677:127–142.
20. Xu C, Wang BC, Yu Z, Sun M (2014) Structural insights into *Bacillus thuringiensis* Cry, Cyt and parasporin toxins. *Toxins (Basel)* 6(9):2732–2770.
21. Jenkins JL, Lee MK, Valaitis AP, Curtiss A, Dean DH (2000) Bivalent sequential binding model of a *Bacillus thuringiensis* toxin to gypsy moth aminopeptidase N receptor. *J Biol Chem* 275(19):14423–14431.
22. Crosa JH (1980) A plasmid associated with virulence in the marine fish pathogen *Vibrio anguillarum* specifies an iron-sequestering system. *Nature* 284(5756):566–568.
23. Lee CT, et al. (2008) A common virulence plasmid in biotype 2 *Vibrio vulnificus* and its dissemination aided by a conjugal plasmid. *J Bacteriol* 190(5):1638–1648.
24. Le Roux F, et al. (2011) Virulence of an emerging pathogenic lineage of *Vibrio nigripulchritudo* is dependent on two plasmids. *Environ Microbiol* 13(2):296–306.
25. Vadivelu J, et al. (1996) Hemolysins and plasmid profiles of *Vibrio parahaemolyticus*. *Southeast Asian J Trop Med Public Health* 27(1):126–131.
26. Kongrueng J, et al. (2014) Characterization of *Vibrio parahaemolyticus* causing acute hepatopancreatic necrosis disease in southern Thailand. *J Fish Dis*, 10.1111/jfd.12308.
27. Soberón M, Gill SS, Bravo A (2009) Signaling versus punching hole: How do *Bacillus thuringiensis* toxins kill insect midgut cells? *Cell Mol Life Sci* 66(8):1337–1349.
28. Pigott CR, Ellar DJ (2007) Role of receptors in *Bacillus thuringiensis* crystal toxin activity. *Microbiol Mol Biol Rev* 71(2):255–281.
29. Coplin DL, Rowan RG, Chisholm DA, Whitmoyer RE (1981) Characterization of plasmids in *Erwiniastewartii*. *Appl Environ Microbiol* 42(4):599–604.
30. Grochulski P, et al. (1995) Bacillus thuringiensis CryIA(a) insecticidal toxin: crystal structure and channel formation. *J Mol Biol* 254(3):447–464.
31. Sambrook J, Fritsch EF, Maniatis T (1989) *Molecular Cloning: A Laboratory Manual* (Cold Spring Harbor Lab Press, Cold Spring Harbor, NY), 2nd Ed.
32. Shao CP, Hor LI (2000) Metalloprotease is not essential for *Vibrio vulnificus* virulence in mice. *Infect Immun* 68(6):3569–3573.
33. Philippe N, Alcaraz JP, Coursange E, Geiselmann J, Schneider D (2004) Improvement of pCVD442, a suicide plasmid for gene allele exchange in bacteria. *Plasmid* 51(3):246–255.
34. Lightner DV (1996) *A Handbook of Shrimp Pathology and Diagnostic Procedures for Diseases of Cultured Penaeid Shrimp* (World Aquaculture Society, Baton Rouge, LA).
35. Aranguren FL, Tang KFJ, Lightner DV (2010) Quantification of the bacterial agent of necrotizing hepatopancreatitis (NHP-B) by real-time PCR and comparison of survival and NHP load of two shrimp populations. *Aquaculture* 307(3–4):187–192.
36. Otwinowski Z, Minor W (1997) Processing of X-ray diffraction data collected in oscillation mode. *Methods Enzymol* 276:307–326.
37. Terwilliger TC, Berendzen J (1999) Automated MAD and MIR structure solution. *Acta Crystallogr D Biol Crystallogr* 55(Pt 4):849–861.
38. Cowtan K (2006) The Buccaneer software for automated model building. 1. Tracing protein chains. *Acta Crystallogr D Biol Crystallogr* 62(Pt 9):1002–1011.
39. Emsley P, Lohkamp B, Scott WG, Cowtan K (2010) Features and development of Coot. *Acta Crystallogr D Biol Crystallogr* 66(Pt 4):486–501.
40. Vagin AA, et al. (2004) REFMAC5 dictionary: Organisation of prior chemical knowledge and guidelines for its use. *Acta Crystallogr D Biol Crystallogr* 60(Pt 12 Pt 1):2284–2295.
41. Collaborative Computational Project, Number 4 (1994) The CCP4 suite: Programs for protein crystallography. *Acta Crystallogr D Biol Crystallogr* 50(Pt 5):760–763.
42. Carver T, Thomson N, Bleasby A, Berriman M, Parkhill J (2009) DNAPlotter: Circular and linear interactive genome visualization. *Bioinformatics* 25(1):119–120.
43. Hall TA (1999) BioEdit: A user-friendly biological sequence alignment editor and analysis program for Windows 95/98/NT. *Nucleic Acids Symp Ser* 41:95–98.